

COUPLING OF LOWER HYBRID WAVES TO THE ASDEX PLASMA

M. Zouhar, T. Vien, F. Leuterer, M. Muenich, M. Brambilla, H. Derfler,
D. Eckhardt, F. v. Woyna and ASDEX-Team

Max-Planck-Institut für Plasmaphysik, EURATOM Association, D-8046 Garching, FRG

1. Introduction

The ASDEX Lower-Hybrid experiment uses an eight waveguide grill antenna to launch the waves. A mean power reflection coefficient as low as $\langle R \rangle = 0.1$ is attainable in all modes of operation. However the reflection coefficients R_k in the individual waveguides may vary over a great range (up to 0.9). This paper aims at depicting the reflection patterns $R_k = f(k)$ and comparing measurement with theory.

At high power levels (above 140 kW/waveguide) a breakdown occurs. The sequence of phenomena relating to this breakdown is documented and commented on.

2. Calculated reflection patterns

Each of the reflection patterns depicted in the diagrams below consists of eight values R_k (power reflection coefficients) in the individual waveguides. Lines are drawn between adjacent points to render the shapes of the patterns prominent; they have no physical meaning otherwise. The patterns dealt with here all result from equal incident amplitudes in the individual waveguides. In each of the diagrams representing computed data, the plasma density gradient in front of the grill is kept constant and the plasma edge density is considered as a parameter.

The following characteristics are predicted by the theory:

- in general the R_k -patterns are expected to vary fairly sensitively with the plasma edge density. This is true for all waveguide phasings.
- a characteristic transition in the R_k -pattern occurs: at low edge density the edge waveguides exhibit low reflection while in centre waveguides reflection is relatively high ("ridge-pattern"). The opposite is true for high density ("valley-pattern"). In between an intermediate density exists with low reflection in all waveguides (overall $\langle R \rangle = 0.1$).
- symmetric reflection patterns R_k ($k=1..8$, axis of symmetry between waveguides 4 and 5) are expected for waveguide phasings $0\pi 0\pi 0\pi 0\pi$, $00\pi\pi 00\pi\pi$, $00\pi\pi\pi\pi 00$, $0000\pi\pi\pi\pi$. Characteristic "double-ridged" patterns are expected for $00\pi\pi 00\pi\pi$ and $0\pi 0\pi 0\pi 0\pi$ phasings, the "ridges" being in waveguides 3 & 6 and 2 & 7 respectively.
- asymmetric reflection patterns are expected for 90 degrees difference between adjacent waveguides (+90 deg denoted "current drive" phasing, -90 deg "opposite current drive", i.e. opposite to the sense of the OH-current) and for similar phasings (120 deg, 60 deg, etc.).
- the phasings $00\pi\pi\pi\pi 00$ and $0000\pi\pi\pi\pi$ have little importance for plasma heating. However, the accompanying R_k -patterns are very particular and fairly pronounced in magnitude. They offer an additional convenient opportunity to verify the theory.
- the computed R_k -patterns are depicted in Figs. 3a through 7a.

3. Experimental reflection patterns

Good qualitative agreement between experimental and theoretical data was observed:

- the measured R_k -patterns are shown in Figs. 3b through 7b. In most cases data of shots with varying edge density are presented.
- the characteristic shapes of the R_k -patterns are clearly distinguished. Relative plasma density changes in front of the grill were measured by means of a microwave interferometer (at 136 GHz). The R_k -patterns vary with density as anticipated.
- the agreement in magnitude is rather coarse. It should be noted however that no absolute values n_{edge} and V_n were taken. In addition, the theoretical boundary conditions are not really those of the experiment (infinite plane conducting wall surrounding the grill, parallel plate geometry).
- all theoretically symmetric R_k -patterns experienced some experimental asymmetry. Possibly the alignment of the grill relative to the plasma torus was not perfect.

4. Breakdown in front of the grill

At high power levels (above 140 kW/waveguide at low densities) a breakdown in front of the grill was detected. This breakdown was studied in more detail by testing a single waveguide (Figs. 1 and 2).

- at first (time $t = 0$), light is detected by the photo-diode PD1 viewing all along the waveguide into the plasma (Fig. 2, first trace, positive signal).
- coincidentally several phenomena occur:
 - a. A pronounced reflection of RF-power is indicated by directional coupler DC3 (outside the grill vacuum section, trace 3, negative).
 - b. At the grill mouth coupler DC1 and the grill coupler DC2 (both being sidewall couplers within the grill vacuum section, both indicating incident waves, both signals negative) amplitude modulation due to the poor directivity of these couplers is clearly visible. The fact that the DC1-signal exhibits just one trough and one crest implies that the locus of the reflection originates in some distance from DC1 and propagates backward. In passing DC1 it causes the DC1-signal to vanish (trace 5). The same happens later at DC2 (trace 6).
- 250 microseconds after $t = 0$: light appears at photo-diode PD2 viewing perpendicularly into the waveguide (trace 2, positive, plateau resulting from saturation).
- 750 microseconds after $t = 0$: the incident wave is switched off (visible at DC3, trace 3, negative) as soon as light appears at PD3 (arc detector).

A possible explanation of this sequence of phenomena is:

- breakdown at the edge of the grill.
- reflection layer (plasma) moving back to the transmitter at a speed of about 3000 m/s, driven by the combined action of ponderomotive force and the force caused by the local magnetic field gradient.

The physics of the breakdown, however, has not yet been identified.

REFERENCES

- /1/ Brambilla M., Nucl. Fusion 16 (1976) 47
- /2/ Stevens J. et al., Nucl. Fusion 21 (1981) 1259

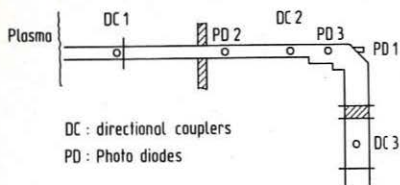
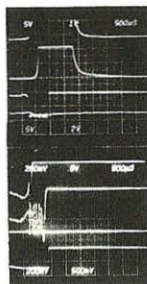


Fig. 1

Breakdown in front of the grill



PD 1
PD 2
DC 3, reflection
DC 1
DC 2
DC 3, incident wave

Fig. 2

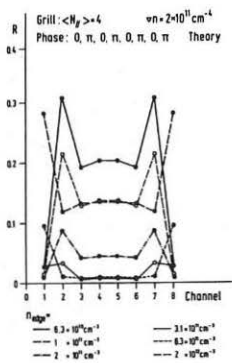


Fig. 3a

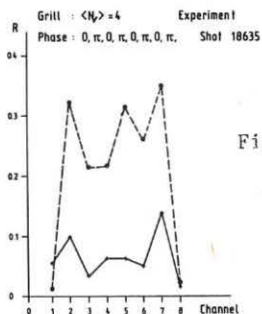


Fig. 3b

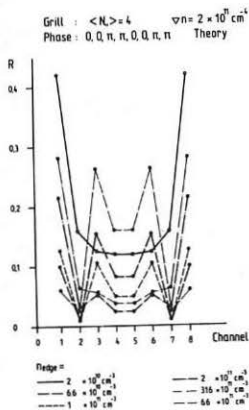


Fig. 4a

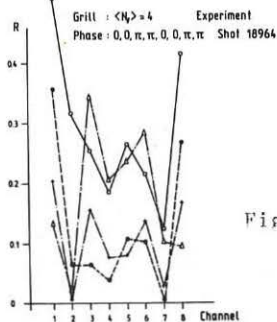


Fig. 4b

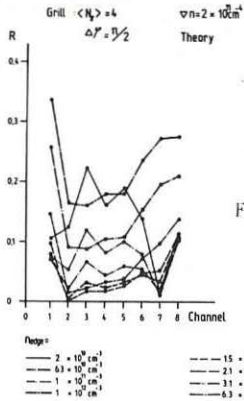


Fig. 5a

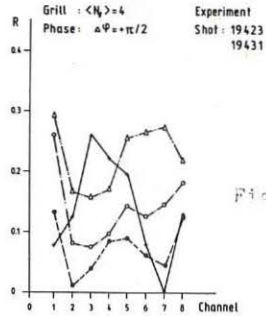


Fig. 5b

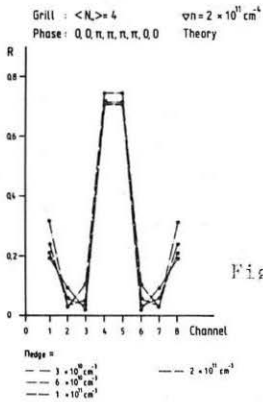


Fig. 6a

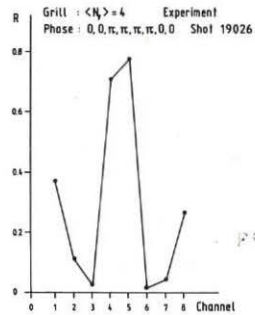


Fig. 6b

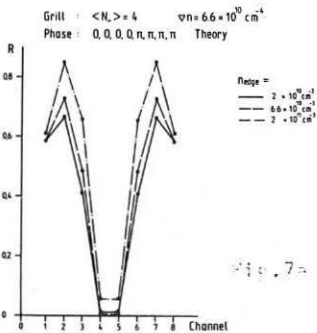


Fig. 7a

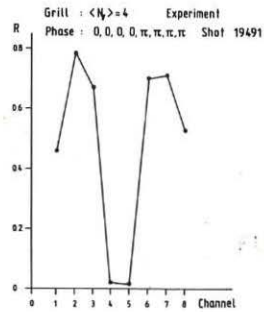


Fig. 7b